Available online at www.sciencedirect.com
SCIENCE DIRECT®
Thermochimica Acta 432 (2005) 135–147
thermochimica acta
www.elsevier.com/locate/tca

Crystallization in ultra-thin polymer films Morphogenesis and thermodynamical aspects

Jens-Uwe Sommer*, Günter Reiter

Institut de Chimie des Surfaces et Interfaces, CNRS-UHA, 15, rue Jean Starcky, B.P. 2488, 68057 Mulhouse Cedex, France

Received 19 November 2004; received in revised form 6 April 2005; accepted 8 April 2005
Available online 24 May 2005

Abstract

We present a computer model for polymer crystallization in ultra-thin films where chains are considered as dynamical units. In our model chains can change their internal state of order by cooperative motions to improve thermodynamic stability. The interplay between reorganization, enthalpic interactions and the morphology of crystals enables us to explain many properties of growth, morphogenesis and melting of polymer lamellae. We emphasize the relation between the thermodynamic stability of non-equilibrium crystals and morphological features which are beyond the average thickness of the lamellae. In particular, we show that melting of polymers is preceded by reorganization processes and the stability of polymer crystals is not necessarily related to the structure formed at the crystallization point. The simulations allow for the determination of some non-equilibrium properties such as the internal energy and the non-equilibrium heat capacity. We show that multiple-peak melting endotherms result from morphological transformations. The results of our computer simulations are compared with AFM observations in ultra-thin polyethyleneoxide films.

PACS: 87.15.Nn; 82.40.Ck; 64.60.−i

Keywords: Polymer crystallization; Computer simulation; Thin films; Meta-stability; Morphogenesis

1. Introduction: the non-equilibrium nature of polymer crystals

The outstanding feature of flexible polymers is their high conformational entropy which is the basis for the understanding of many universal features of polymeric systems and plays an important role for the understanding of material properties of soft-matter. A long chain molecule may be even considered as a small thermodynamic system where the entropy is related to the many conformational degrees of freedom (typically an exponential function of the chain length). During crystallization a great part of this conformational entropy has to be reduced and the resulting crystal has to obey strong constraints due the linear connectivity of crystallizing units. As discovered by Keller [1], Till [2] and Fischer [3] polymers crystallize in form of lamellae which are usually much thinner compared to the fully extended chains. Therefore, every chain has to transverse many times through the lamella thus leading to the picture of folded chain crystals, see left part of Fig. 1. The thickness of these crystalline lamellae is usually of the order of 10 nm while its lateral extension can be hundreds of μm. Since the surface free energy of the fold-surfaces (top and bottom surfaces of the lamella) is much higher that that of the lateral surfaces such a structure cannot be the equilibrium form of the polymer crystal [4,5]. A thicker lamella corresponds to a lower free energy and thus lamellae containing fully extended chains are thermodynamically optimal. In fact, for short *n*-alkanes [6] up to a length of about 150 CH_2-units and for polyethylene under high external pressure extended chain crystals can be observed. In the latter case this happens because of the high mobility in the hexagonal phase of polyethylene chains under high pressure/temperature conditions [7]. Thus the extended chain form is not obtained in equilibrium with the melt but due to a specific kinetic pathway from starting with an undercooled melt.

* Corresponding author. Tel.: +33 3 8960 8722; fax: +33 3 8960 8799.
E-mail address: ju.sommer@uha.fr (J.-U. Sommer).

0040-6031/$ – see front matter © 2005 Elsevier B.V. All rights reserved.
doi:10.1016/j.tca.2005.04.017

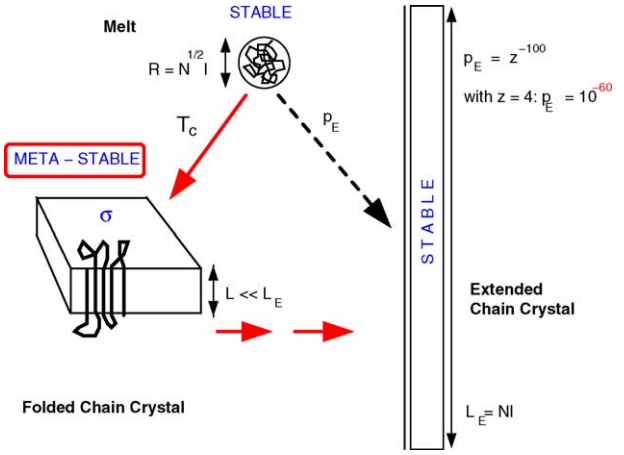

Fig. 1. Sketch of the different phases of a polymer chain. In the melt all possible chains conformations are realized which results in average in a random coil-like shape. In the hypothetical equilibrium state of the crystalline lamella only the stretched chain conformation is realized which corresponds to an enormous decrease of entropy per molecule. The meta-stable lamella is formed by partially stretched chains and at a substantial undercooling.

In order to understand the appearance of meta-stable folded-chain lamellae instead of extended chain lamellae we imagine a phase equilibrium between an extended chain crystal and the corresponding melt. At the hypothetical phase equilibrium detailed balance conditions have to be obeyed. Chains from the melt phase can join the crystal phase with the same rate as chains leave the crystal phase. Moreover, at the true phase coexistence no intermediate states will be favored such as partially folded states. In fact, such states have a lower melting temperature which destroys the reversibility. The situation is sketched in the right part of Fig. 1. The particular problem for chain molecules is now that all crystal units have to be arranged exactly in a straight array and cannot be attached at random points on the growth front. This corresponds to a huge entropy reduction per chain attachment. In the melt phase the chain attains a random coil conformation which corresponds to a typical spatial extension of $R = l\sqrt{N}$, where l denotes Kuhn's segment and N is the number of Kuhn segments in the chain. This corresponds to the state where all possible conformations of the chain can be obtained with equal probability. The number of these conformations can be expressed as

$$Z = z^N, \tag{1}$$

where z denotes the (effective) coordination number (number of orientational states) of each segment. The probability to realize the fully extended chain conformation is therefore given by $p_0 = 2/Z$. Assuming a chain of only 100 units and a coordination number of $z = 4$ we obtain the unphysical small number of about $p_0 = 10^{-60}$. By taking into account a molecular time scale of about $t_0 = 10^{-12}$ s we obtain for the average time of fluctuation from the melt state to the crystalline state: $t = 10^{48}$ s which corresponds to about 10^{40} years. This calculation example shows that detailed balance conditions (and hence a true phase coexistence) may be impossible.

However, if the system is substantially supercooled (up to hundred Kelvin and more) partially ordered chain conformations which can be reached rather easily from the disordered state at the growth front can be stable enough to allow for further growth. In this way only part of the entropy of the chain has to be reduced. The resulting lamellar is then much thinner compared to the extended chain crystal as sketched in the left part of Fig. 1 and will be denoted as folded chain crystals. Because of the excess surface tension of folded chain crystals they are only meta-stable. Spontaneous thickening processes which increase the degree of order of each chain yield to crystal forms of increasing thermal stability.

The problem emerges of how to characterize the meta-stable state of polymer lamellae. In thermodynamic equilibrium the temperature T is the only control parameter if the external pressure is not varied. Non-equilibrium states, however, require the introduction of additional variables in order to characterize them uniquely. These additional variables represent all information about the history of a non-equilibrium system necessary to reproduce a given state uniquely [8]. The traditional representation of the state of polymer lamellae is the diagram which is displayed in Fig. 2. Here, the averaged thickness of the lamella L is taken as the only relevant information about the state of the lamella. Note, that L cannot be adjusted externally *independent of temperature* but is just the consequence of a particular temperature protocol applied to the system.

The states in Fig. 2 have to be understood in the following way. First, a true equilibrium state in the disordered phase has to be prepared (liquid state at a temperature well

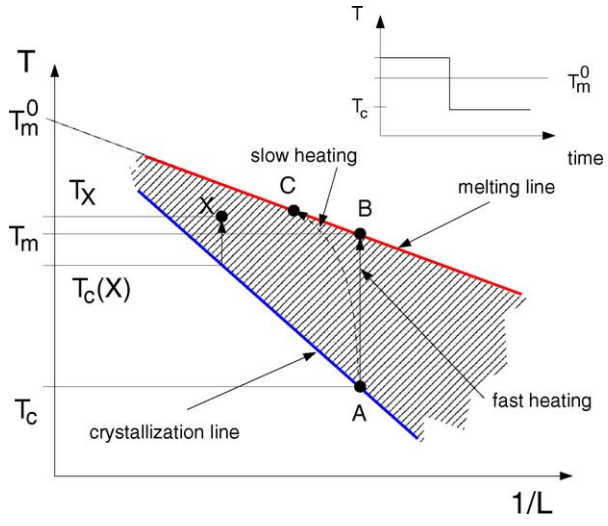

Fig. 2. Sketch of the standard non-equilibrium state diagram for lamellar crystals. States are characterized by the temperature T and the inverse average lamellar thickness $1/L$. Only the hatched region between the crystallization line and the melting line is physically accessible. The lamellar thickness represents the history of the polymer crystal.

above the melting temperature). Then, the system is rapidly quenched into an unstable state where crystal growth starts. The corresponding temperature protocol is shown in the upper right part in Fig. 2. The crystallization temperature T_c leads to the selection of a meta-stable lamella thickness $L(T_c)$ which is observed immediately after the quench and is represented by a single point (state A) in the diagram in Fig. 2. Fast heating leads to fusion at a higher temperature T_m (state B). Performing a series of experiments with different values of T_c yields the *crystallization line* and a corresponding *melting line* in the state diagram. Linear extrapolation of the melting line towards $1/L \to 0$ defines the so-called *equilibrium melting temperature* T_m^0. It is obvious that only states between the crystallization line and the melting line have a physical meaning in the state diagram (hatched area).

So far, the history the system, given by the temperature protocol $T(t)$, where t denotes the time, has been chosen to obtain a constant value of L. However, slow heating of lamellae crystallized in state A can lead to other states in the state diagram and to fusion at a higher temperature, denoted as state C in Fig. 2. Under such a temperature protocol irreversible thickening of the lamella can take place. This is illustrated in Fig. 3 by experimental results on isotactic polystyrene obtained by Al-Hussein and Strobl [9]. Note that the range between crystallization and melting temperature can be higher than 100 K and the difference between the lowest crystallization temperature and the extrapolated equilibrium temperature is almost 200 K. The data where obtained by stepwise heating and annealing the crystallized polymer.

We note again that the variable L cannot be controlled independently of T like a thermodynamic variable but results from the history $T(t)$. Furthermore, only changes in one direction of L are possible. It is not possible to drive back the system in the state diagram once a change of L has taken place without leaving the crystalline state. To emphasize the difference to equilibrium phase diagrams we consider some state X in the inner part of the physical region of the state diagram, see Fig. 2. It is not possible to reach this state directly by adjusting a few external parameters. Rather it is necessary to find a temperature protocol which drives into X passing over other states which are not on the left side of X in the state diagram. One possibility is to quench from the melt to the temperature $T_c(X)$ followed by a rapid heating to T_X. In any case a definite *kinetic pathway* must be applied to obtain a non-equilibrium state X.

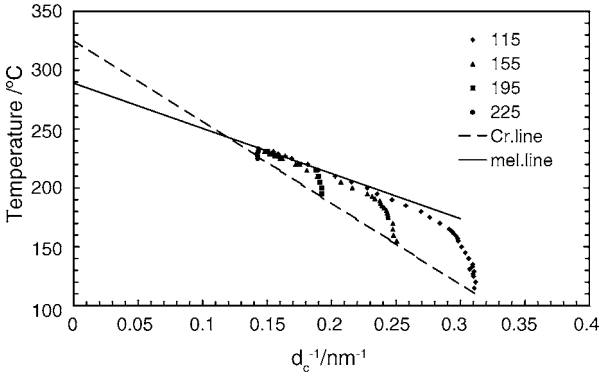

Fig. 3. Non-equilibrium states of isotactic polystyrene of molecular weight of 400 kg/mol. A variation of the L (here denoted as d_c) is clearly observed during stepwise heating [9].

It is widely believed that the melting line corresponds to a simple Gibbs–Thomson like melting-point depression due to excess free energy of the fold-surface, see [10]. A first-order thermodynamic expansion around the melting point of an infinitely thick crystal, T_m^0, leads to

$$\frac{T_m^0 - T_m}{T_m^0} = \frac{1}{L}\frac{2\sigma_F}{q}, \tag{2}$$

where σ_F denotes the excess free energy of the fold surface (the lateral surfaces can be neglected) and q denotes the heat of fusion per unit volume Q/V. This equation corresponds to a straight line in the state diagram: $T_m = T_m^0 - c(1/L)$, where the slope c is given by $c = 2T_m^0\sigma_f/q$. A true thermodynamic equilibrium is assumed at the melting point with a *fixed* lamellar thickness L.

In Fig. 4 we illustrate the difference between the original Gibbs–Thomson problem of melting a small spherical object and the present case of an extended non-equilibrium lamella. A sphere, Fig. 4a, corresponds to the optimal thermodynamic shape of an isotropic object. Therefore, the stability limit is fairly well expressed by the thermodynamic argument which includes the surface free energy excess. On the other hand, a laterally extended thin lamella corresponds to a thermodynamic unfavored shape. Close to the stability limit morphological changes, see Fig. 4b, can lead to more stable intermediate phases before the system melts at a higher melting temperature. As illustrated in Fig. 4b also a break-up into smaller but thicker objects might be thermodynamically favored. Only a very fast heating process would avoid such morphological changes. In this case, however, kinetic super-heating effects might overlay the Gibbs–Thomson stability limit. For all these reasons, a simple equilibrium thermodynamical explanation of the melting line according to Eq. (2) might be wrong. At this point it should be added that until now no experiments are known to the authors where the excess free energy of the fold surface of a single crystal has been measured directly. Moreover, it is by far not clear whether the excess free energy corresponds to the surface tension as it could be measured for instance in dewetting experiments.

The diagram in Fig. 2 suggest that states of polymer crystals are uniquely described by the temperature and the lamellar thickness. In other words: the average lamellar thickness is sufficient to characterize all history effects in polymer crystallization. In Section 3 we will show that more than one length scales are necessary to characterize non-equilibrium growth structures as they are observed in thin polymer films.

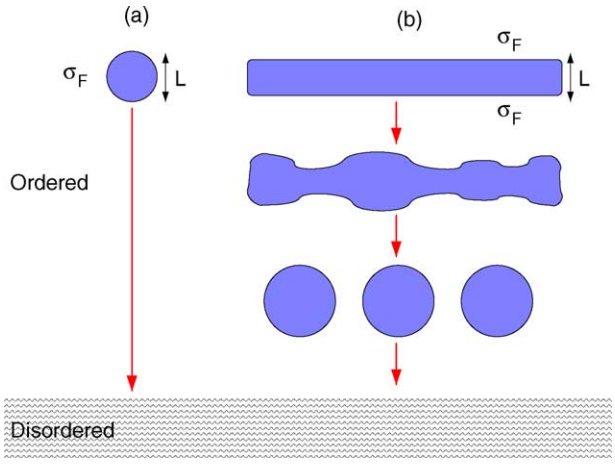

Fig. 4. Gibbs–Thomson effect and morphological changes. (a) Melting temperature of a sphere at the thermodynamic stability limit depressed by the surface free energy. (b) A thin but laterally extended lamella does not correspond to the optimal thermodynamic shape. Morphological changes can lead to more stable phases which melt at higher temperatures. Therefore, the final melting temperature is not directly related to the surface free energy in the state of formation of the crystal but could be related to the surface free energy of the morphology after possible reorganization processes.

2. The role of internal chain order

When a molecule crystallizes in a simple liquid it has to reduce its translational and rotational degrees of freedom as sketched in the right part of Fig. 5. The internal state of the molecule is invariant. By contrast, when a long chain molecule crystallizes it has to undergo an *internal transition* from the disordered state to the ordered state. This is illustrated in the left part of Fig. 5.

Considering the chain as the crystallizing unit, a polymer crystal is a super-crystal consisting of ordered single-chain crystals. In previous models this point has been usually ignored. In the model of Hoffman and Lauritzen [4] stems are considered as elementary units which correspond to the

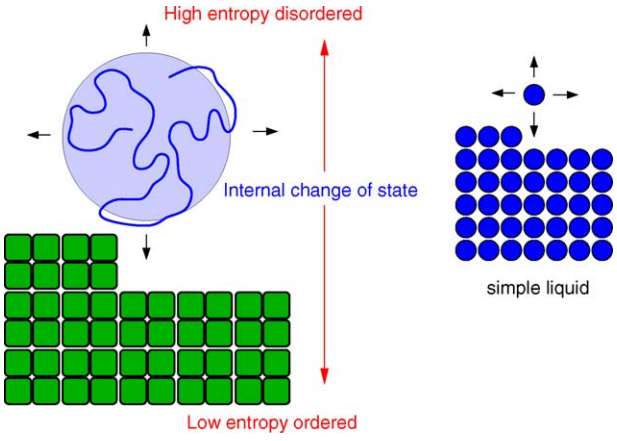

Fig. 5. Qualitative difference between the crystallization of polymers (left part) and low molecular liquids (right part).

stretched parts of the chain in the crystal phase. However, experimental as well as theoretical arguments have shown that stems of the same chain do not appear in a random arrangement in the crystal. Such a disorder would result in a so-called random switchboard structure of the fold surface where amorphous loops connect stems which are not in neighboring places. For single crystals various studies give strong indication for a regular arrangement of folds which implies that single chains form a connected fold structure [11].

Note that the formation of regular folded chains *is assumed* in the HL-model but does not follow from the idea of secondary nucleation itself. The fact that stems recognize their neighbors along the chain is nothing else than a manifestation of cooperativity of the chain in the crystallization process. Sadler and Gilmer [12] (SG) have proposed an alternative model where cooperativity is required for each stem but monomers are considered as independent units. This model neglects any lateral correlations on the growth front and thus cannot make any prediction about order beyond the size of a single stem. On the other hand, the SG-model addresses for the first time the entropic nature of chain ordering during growth. Both models have in common that they try to explain the process of selection of lamellar thickness by considering stems as basic units. The role of the chains in polymer crystallization was first appreciated for short chains such as *n-alkanes*. Simple assumptions about cooperative chain motions (expressed by certain kinetic pathways of chain folding and stretching) has been successfully applied to explain the self-poisoning behavior of *n-alkanes* (decrease of growth rate with temperature) [13] and the unusual behavior of binary mixtures of short and long *n-alkanes* [14].

In all what follows, *we will assume the crystallization requires cooperativity of the whole chain*. Moreover, we will characterize the state of a single chain by an order parameter which can take different values in the crystalline phase according to the different degrees of stretching of the whole chain. This idea is illustrated in Fig. 6. Our aim is to model polymer crystallization by considering chains as elementary objects which can be in various ordered states characterized by an order parameter m. The disordered state corresponds to $m = 0$. To reach an ordered state an entropic barrier has to be overcome which corresponds to a probability p_S to increase the internal order in each time interval typical for the fluctuation of the chain. The special features of polymer crystals are obtained by the interplay between internal order of each chain and the interaction with other chains in the crystal. The higher the internal degree of order of the two neighboring chains, the stronger is the coupling in the crystal. On the other hand, to reach a high degree of internal order a long time is passed in lower states of order. Therefore, at the crystallization temperature a kinetic selection of the average degree of chain order (lamellar thickness) takes place and results in lamellae which are stable enough to grow but avoid higher order. Nevertheless, further reorganization into better ordered states is possible. The latter will be important close to the stability limit of the lamella.

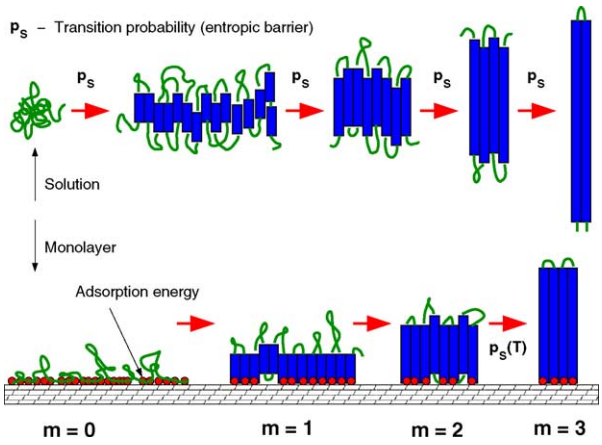

Fig. 6. Illustration of different degrees of internal chain order which defines the order parameter m. For simplicity we characterize the order parameter with an integer value. Increasing the chain order requires entropy reduction which corresponds to some probability p_S. When crystallization takes place on substrates increasing the internal order involves energetic interactions. If adsorbed and non-adsorbed chains are present it might be necessary to distinguish between $m = 0$ and $m = 0+$ to indicate the adsorbed, amorphous state, $m = 0+$, explicitly. This will be no the case in the present work.

3. Crystallization in ultra-thin films

In recent years there is growing interest in thin and ultra-thin polymer films. Here, "ultra-thin" indicates a film thickness of the order of the radius of gyration of the chains. This may correspond to a monolayer. In ultra-thin polymer films an external nucleation site is always required to spawn a crystallization process [15]. Homogeneous nucleation is highly suppressed. Typically, diffusion controlled growth pattern can be observed which correspond to polymer lamellae growing flat on the substrate. An example is shown in Fig. 7 for ultra-thin films of polyethyleneoxide (PEO) of molecular mass of 7.6 kg/mol.

In order to obtain ultra-thin polymer films dewetting processes are used. At temperature above 70 °C holes are formed on the substrate, see the upper part of Fig. 7. Because of the strong adsorption of PEO chains on the silicon waver this corresponds to so-called autophobic or pseudo-dewetting leaving a mono-layer of adsorbed molecules behind. Closer investigation reveals finger-like crystal structures inside the holes which are formed by cooling the sample below 60 °C, see Fig. 7A. The 3D representation of part of the finger-structure given in Fig. 7B shows two relevant length scales of the pattern. The height h which corresponds to the lamellar thickness L and the width of the fingers w. We obtain $h \simeq 8$ nm which corresponds to a multiple folded chain structure. The width of the fingers is in the range of μm. More details can be found in Refs. [16,17].

The growth morphology of polymer crystals obtained under diffusion control has to be characterized by several length scales as illustrated in Fig. 8. As discussed above, in addition to the lamellar thickness there appears a characteristic width of fingers w. Moreover, a correlation length ξ

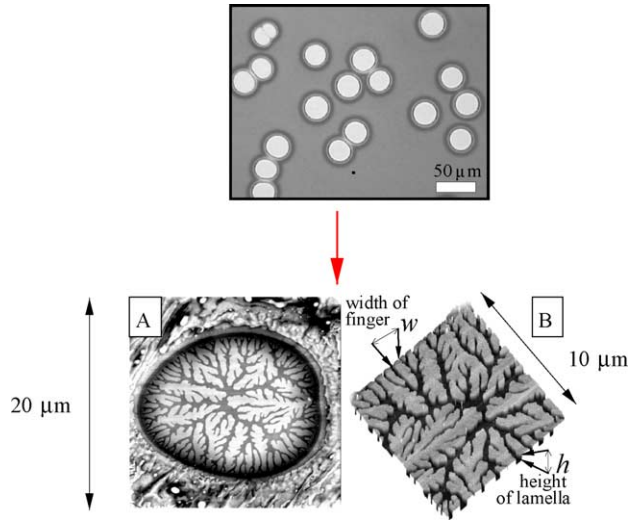

Fig. 7. Crystallization in ultra-thin polymer films. The upper figure shows an optical micrograph of a typical dewetting pattern in a thin PEO film (thickness about 100 nm). The white circles represent the holes containing a molten monolayer resulting from pseudo-dewetting. The lower part shows the result obtained by tapping mode AFM (topography). Finger-like growth patterns are obtained after crystallization for 880 min at 44 °C in a pseudo-dewetted hole. (A) Fingers inside the hole (image flattened to enhance the visibility of the fingers). All fingers start at the periphery of the hole. (B) 3D representation of fingers in (A).

can be introduced which characterizes the average distance between the fingers. The correlation length can be related to the jump in the 2D density between ultra-thin amorphous layer and the crystalline lamella [18,19].

Polymer crystallization in quasi-two dimensions allows a direct investigation of the crystal morphology using AFM-techniques. The thickness of the lamellae are directly obtained in height images. Moreover, the local crystal thickness becomes visible and non-trivial morphological features can be studied as will discussed below. Complications due to multi-lamellar structures and 3D-morphologies (spherulites) are avoided in 2D crystallization and single lamellar structures can be observed in situ under the treatment of various

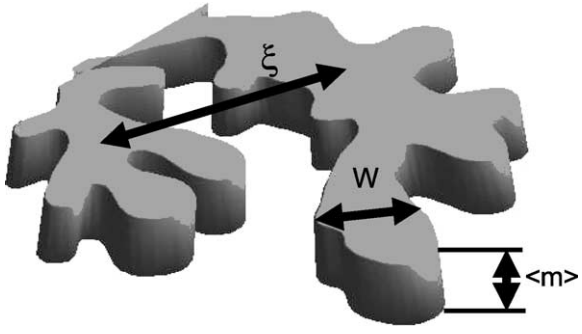

Fig. 8. Illustration of three relevant length scales for polymer crystals created under diffusion control. The average height $\langle m \rangle$ corresponds to the lamellar thickness L. In addition, individual fingers have a characteristic width in the range of 100 nm to μm. Dense branching morphologies obtained in Fig. 7 display a correlation length ξ.

temperature protocols. The great advantage of these systems is that they allow for a simple modeling on the scale of polymer chains.

4. A generic algorithm for polymer crystallization in ultra-thin films

How can crystallization from a dense polymer layer lead to diffusion controlled patterns? The answer to this question is related to the fact that lamellae grow at greater height than the amorphous film. In order to join the lamella at the growth front the adsorbed chains have to desorb partially to form upright folded states, see Fig. 9a. This way the surface area occupied by a single chain changes from A_0 (disordered state) to A (ordered state). Directly at the rims of a pseudo-dewetted hole (which serve as nucleation sites) the crystal starts to grow. When growth proceeds a depletion layer is created due to the emergence of more and more unoccupied surface places. As a result, diffusion control sets in as illustrated in Fig. 9a. Moreover, the order parameter m can be defined as the ratio of the two surface areas as follows

$$m = \frac{A_0}{A}. \tag{3}$$

This is illustrated in part (b) of Fig. 9. Note that this order parameter corresponds to the degree of internal order as defined in Section 2, see also Fig. 6 and denotes the number of ordered chains which can be accumulated within the area covered by a single disordered chain, see Fig. 9c.

The advantage of 2D polymer crystallization is therefore the simple mapping of the degree of internal chain order to an order parameter which is directly related to the increase of occupation of chains per surface area unit due to crystallization. This enables us to define a simplified lattice algorithm in which chains can be treated as basic units. The idea of our algorithm is displayed in Fig. 10. We consider a quadratic lattice where the lattice constant corresponds to the extension of adsorbed 2D chains, i.e. $A_0 \sim N$. These chains can move on the lattice (substrate) respecting excluded volume effects. Note that chains in 2D can be considered as non-interpenetrating disc-like objects. In the crystalline state we allow for multiple occupation of lattice cells according to our considerations above, see Fig. 9c. In order to stay on the scale of the lattice constant we assume for simplicity that all chains which share the area of A_0 are in the same state of order.

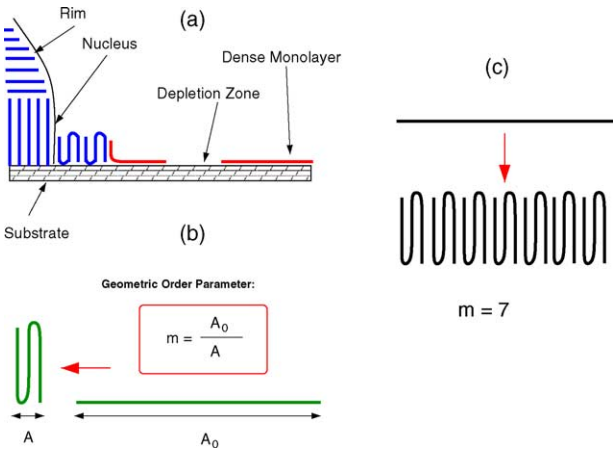

Fig. 9. Illustration of the growth process in ultra-thin films. (a) To join the (flat-on oriented) lamella, chains must achieve an upright (folded) conformation. (b) Transition from flatly adsorbed to upright folded states changes the occupied surface area A. An order parameter can be defined by the reduction of occupied surface area. (c) The area occupied by a single liquid chain can be occupied by m ordered chains. The corresponding reduction of overall occupied area results in a depletion zone at the growth front as illustrated in (a).

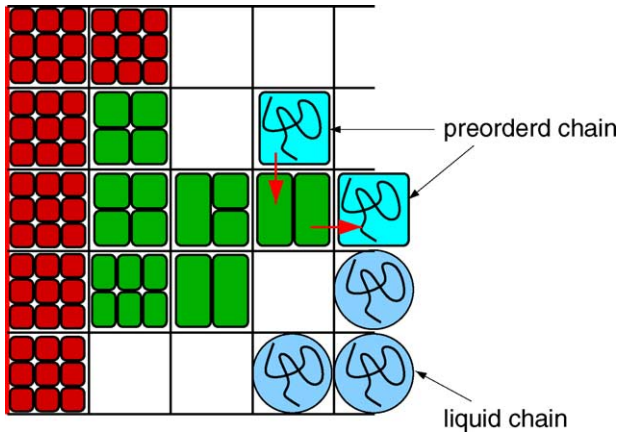

Fig. 10. Generic lattice model for crystallization in ultra-thin films. In order to stay on the scale of adsorbed liquid chains we map a higher degree of order into a multiple occupation on the lattice (lateral squeezing of chains). All chains in one lattice cell are considered as equivalent with respect to their internal degree of order m. Growth is nucleated by a row of cells with the maximum degree of order.

If a liquid chain touches the growth front, it strongly adsorbs onto it. In this state, the chain conformation is already partially ordered (pre-ordered) and we denote this state as $m = 1$. To join the crystal truly the chain can further increase its internal order in thermal fluctuations by entering a neighboring crystalline cell. Then, the degree of order in this cell is increased by one unit. (In our coarse grained model, this means that all chains occupying this cell must increase their internal order.) Alternatively, two pre-ordered chains can join and form a *new* crystalline cell with $m = 2$. This realizes a growth event at the crystal front. On the other hand, chains at the growth front can return to the liquid state by breaking the crystalline bonds in thermal fluctuations. This will be much easier for chains having a low degree of order, i.e. fewer bonds. The balance between growth events and detachment events determines the overall growth rate. For higher temperature higher degrees of chain ordering will be necessary in order to achieve stable growth. Moreover, by applying a full Monte Carlo scheme we will allow for fluctuations of chains between different cells in the lattice.

Some remarks are necessary about the role of pre-ordered states in our model. As discussed in Section 1, polymer liquids always have to be strongly super-cooled for crystallization to take place. In solvents, this implies a segregation transition if the local concentration (at the growth front) exceeds a certain value, thus leading to strong adsorption at the growth front. But also for the case of crystallization from ultra-thin films a strong interaction between the crystal and liquid chains can be expected. When the chains are adsorbed at the growth front (more precisely in the niche formed by the crystal edge and the substrate) the underlying crystalline lattice provides a periodic potential where the adsorbed chains try to fit in. Thermal fluctuations can lead to higher order and the chain becomes part of the crystal. The ordering process of single chains on crystalline surfaces has been studied in molecular dynamics simulations by Yamamoto [20]. We believe that pre-ordering at the growth front is a very important step since it can explain why spontaneous formation of nuclei are not observable but fluctuations into the ordered state at the growth front take place easily.

Crystal interaction is established between nearest neighbor cells. The more a chain is stretched the higher is the interaction energy, E, with neighboring chains and the more stable is the crystal. On the other hand, to obtain a high value of m a high entropic barrier, see Fig. 6, has to be surmounted. In order to understand the generic properties of the crystallization process we make the most simple assumptions as follows: The interaction energy is given by the minimum of the occupation numbers in nearest neighbor cells m and m'

$$E(m, m') = \epsilon \min(m, m'), \tag{4}$$

where ϵ denotes the interaction energy per unit of the order parameter. If a cell has a higher degree of order compared to the neighboring cell this results in additional excess free energy of the fold surface. Therefore, only the minimum of the order parameter in both cells is accounted for. We introduce a temperature variable T as follows

$$p_0 = \exp\left\{-\frac{\epsilon}{kT}\right\}. \tag{5}$$

If we take the unit of the temperature as ϵ/k, where k denotes Boltzmann's constant, we obtain

$$T = \frac{1}{\ln(1/p_0)}. \tag{6}$$

The thus defined temperature variable is a measure for the local binding of the crystal under thermal agitation. The probability to leave a lattice cell r is then given by summing up over all nearest neighbors:

$$p_r = \sum_{\langle r,r'\rangle} p_0^{\min(m,m')} \tag{7}$$

where the dashed variables run over nearest neighbor sites of r. Note that we always assume that crystal bonds to the neighboring chains have to be broken if a chain later on changes into another crystal cell where such bonds are again established.

For the barrier against ordering we define the following simplified relation

$$\bar{p}(\Delta m) = p_S^{\Delta m}, \tag{8}$$

where p_S is the transition probability to increase the order parameter by one unit. Here, Δm denotes the difference in order between the new cell and the old cell. If this difference is negative, $p(\Delta m)$ is set to unity. Hence, the probability to join a neighboring lattice cell is given by

$$\bar{p}_{rr'} = p_S^{m'-m}. \tag{9}$$

Putting everything together, we obtain the total probability for a move from r to r' as

$$p(r \to r') = p_r \bar{p}_{rr'}. \tag{10}$$

We apply a Monte Carlo procedure. For each step, a chain and a direction for the move are randomly chosen. Then, it is checked whether the move is blocked by ultimate constraints (excluded volume for free chains, maximum occupation M for crystalline cells). If this is not the case, the move is taken with the probability given in Eq. (10) using the Metropolis prescription. The only peculiarity is for the case when a free chain's move is rejected from a crystalline cell. Then, the cell actually hosting the chain (which is next to the crystal front) is transformed into the pre-ordered state $m = 1$ without any penalty, see Fig. 10. Hence, a "contact" to the crystal growth front is required in order to form a pre-ordered state. A Monte Carlo step (MCS) is defined as the time needed to move all Monte Carlo objects (chains, in our case) once on average. The usual time scale which we use in the following are thousand MCS, denoted by TMS.

Since spontaneous nucleation in ultra-thin polymer films is highly suppressed, a primary nucleation site must be provided to observe crystallization effects. In many of our simulations we use a full line of lattice cells occupied with chains of maximum order $m = M$. This mimics the rim around a dewetted hole in the experimental situation, see Fig. 7. In most cases we use full periodic boundary conditions. Therefore, growth starts on both sides of the lattice simultaneously.

In most of the simulations we use a fully occupied lattice as starting condition ($m = 0$) which corresponds to a compact liquid film. Therefore, at the beginning of the simulation only moves which increase the occupation number at the growth front are possible. However, during growth a diluted zone builds up ahead of the growth front. This zone is responsible for the formation of diffusion controlled growth morphologies.

To conclude this section we have proposed a simple lattice algorithm which mimics the growth and reorganization processes during polymer crystallization using polymer chains as dynamical units.

5. Isothermal growth and reorganization in 2D

Our lattice model is controlled by two parameters: The binding energy per ordered unit, expressed by the temperature variable T, see Eq. (6), and the penalty for increasing the order by one unit, given by p_S. In addition, we always consider a maximum value of the order parameter M (which corresponds directly to the length N of the fully stretched chain).

Typical growth morphologies which result from our model are displayed in Fig. 11. Here, p_S is taken as unity (no penalty against conformational order). This results in filling-up of crystalline cells until M is reached. For $T = 0$, see Eq. (6) the growth-process is locally irreversible and chains rest at the place where they entered the growth front. As a result, we obtain a fractal-like growth morphology, where the thickness of the finger-structure corresponds to a single lattice unit, see Fig. 11a.

If the system grows at finite temperature, chains can also leave a crystalline cell which results in a finite width, w, and more compact growth morphologies. Also, the growth rate is rapidly decreasing if the temperature is increased. These effects can be observed in Fig. 11b and c.

Fourier-space analysis [21] reveals that the effect of finite temperature is to erase the higher wavelength contributions of the pattern in favor of a dominating wavelength of the growth morphology. The different characteristic length scales of morphologies for polymer crystals are illustrated in Fig. 8. The Fourier analysis shows that the correlation length ξ, which corresponds to the average distance between

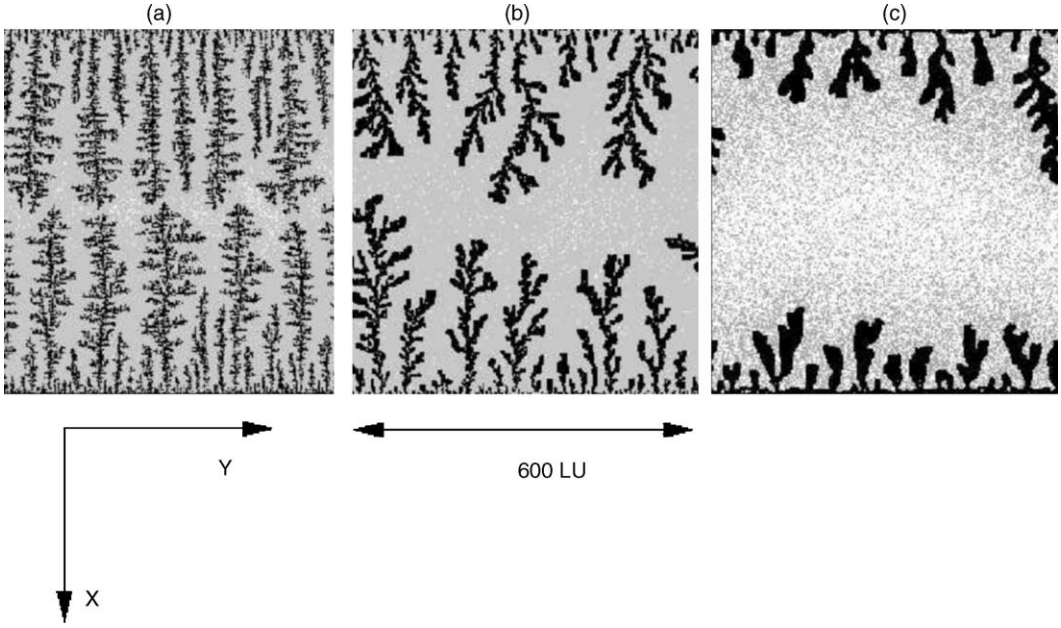

Fig. 11. Typical growth patterns obtained from simulations without penalty against ordering ($p_S = 1$). The lattice size is 600 × 600. (a) Locally irreversible growth with $T = 0$ after 30 TMS. (b) $T = 0.83$ after 60 TMS. (c) $T = 1.44$ after 60 TMS.

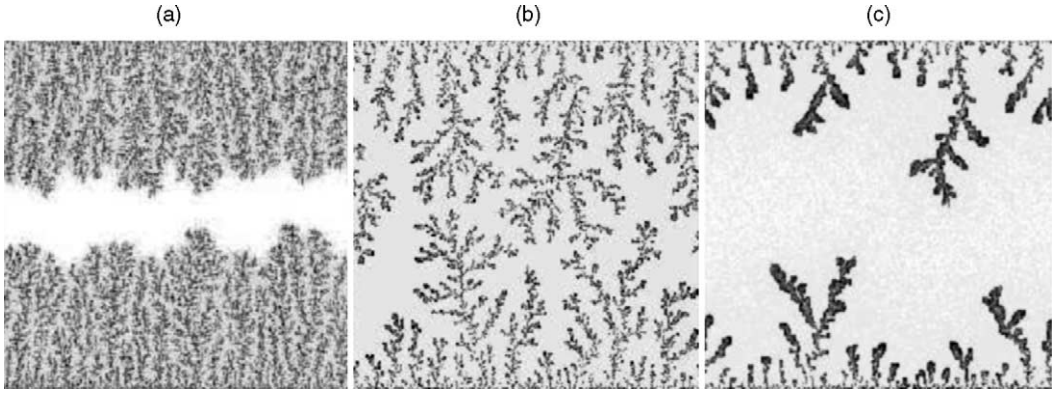

Fig. 12. Growth morphologies for a finite entropic penalty, $p_S = 0.6$. The order parameter is coded in gray scales where darker spots correspond to a higher degree of ordering. (a) Locally irreversible growth $T = 0$. (b) $T = 0.72$ after 30 TMS. (c) $T = 0.95$ after 30 TMS.

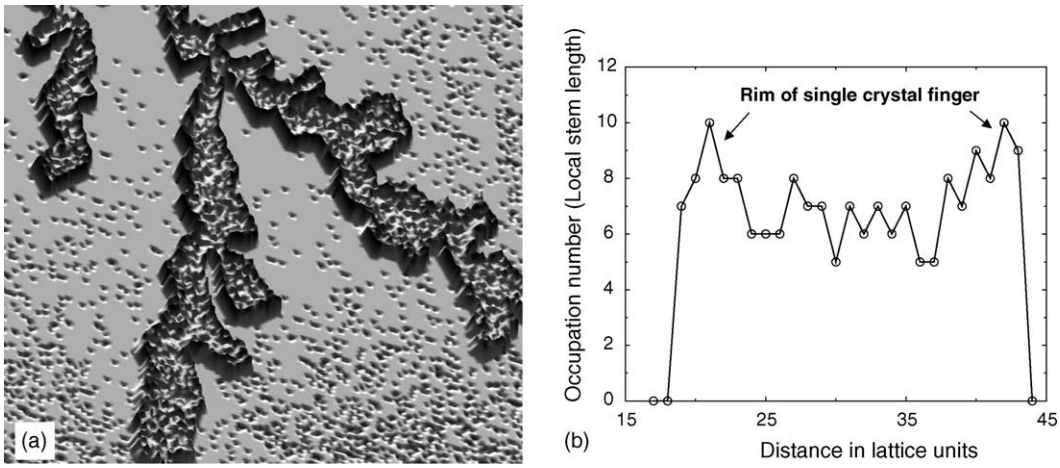

Fig. 13. Part of the growth pattern for $p_S = 0.6$ and $T = 0.95$. (a) 3D representation of crystal structure. (b) Height profile across a finger.

the fingers, is not very sensitive to temperature effects. On the other hand, the finger width w depends strongly on temperature, as can be seen from Fig. 11, see also Ref. [16].

In Fig. 12 we show the effect of a finite penalty $p_S = 0.6$ for increasing the internal chain order. Now, the lamellar thickness $L = \langle m \rangle$ becomes an important parameter, see Fig. 8. The different degrees of order m are mapped into a gray scale, where darker points correspond to better ordered chains (larger L, higher occupation). One clearly observes the increase of L with temperature.

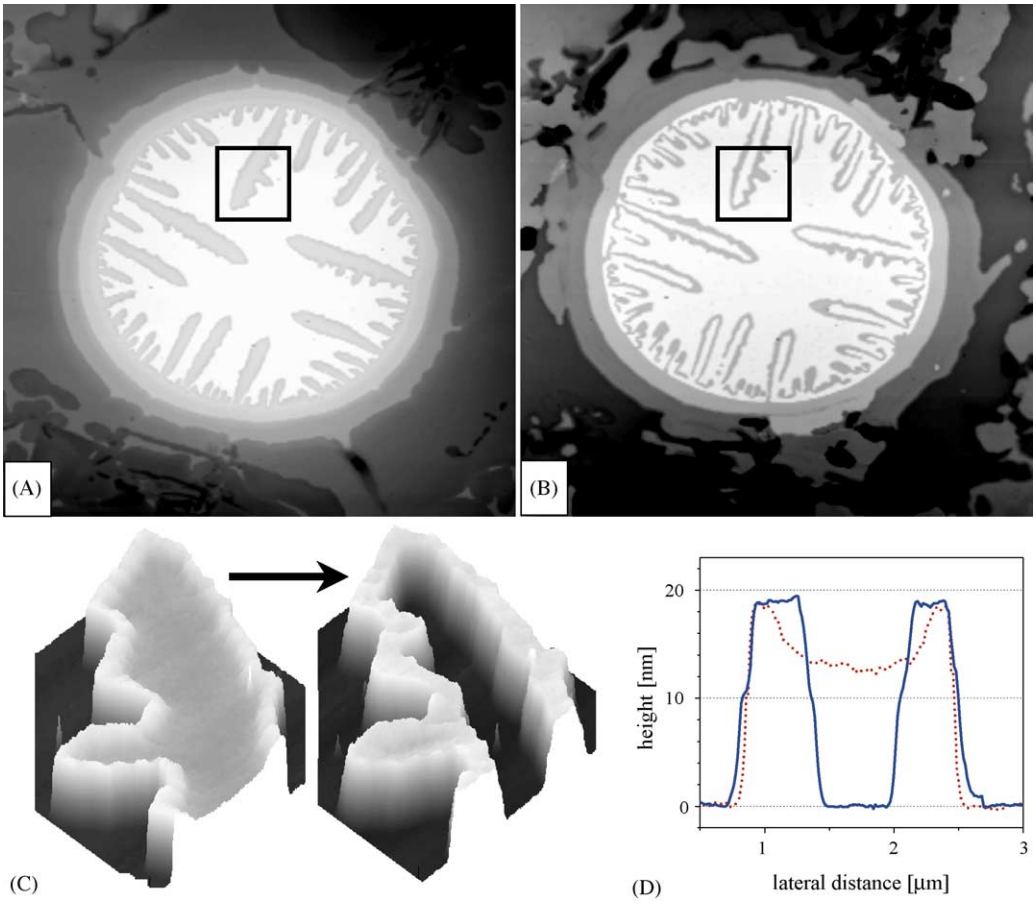

Fig. 14. Tapping mode AFM images showing the morphological changes induced by annealing fingers obtained by crystallization of monolayers of PS-PEO(3k–3k) resulted from pseudo-dewetting, see Fig. 7: (A) after crystallization at 45 °C, (B) after subsequent annealing for 1 min at 54 °C. The size of the images is 40 μm × 40 μm. Parts (C) and (D) show 3D-plots and cross-sections, respectively, from the small square indicated in (A) and (B). The dotted and the full lines in (D) represent the states (A) and B before and after annealing, respectively.

The most striking observation in our model are pronounced reorganization effects of the growth patterns (lamellae) during and after the growth process. At finite temperature chains do not obtain states of maximum order but a compromise between stability and growth velocity is manifested. However, chains located directly at the growth front are quite mobile, i.e. are able to leave there original places.

In Fig. 13 we show the topography of a part of the growth pattern as obtained for $T = 0.95$ after 30 TMS, see Fig. 12c. The edges of the fingers are higher than the interior indicating a higher order at the boundaries of the fingers. The height profile across a finger is shown in Fig. 13b. Closer inspection of the lower part of Fig. 13a indicates that the tip of the longest finger (which reaches deeper into the reservoir of free chains) does not yet exhibit this feature. A fact indicating that the formation of higher ordered edges takes place after growth when the density of free chains is already reduced. This observation is a very general feature of our model which allows for reorganization processes during and after growth. A simple calculation reveals a factor of about 500 between the number of reorganization events at the crystal boundary and the interior of the crystal. For chains having only two or one nearest neighbors (edges) the factor raises up to 300,000 and 160,000,000, respectively for the given set of parameters [22]. On the other hand, the rim-enhanced phase is very stable against further reorganization at isothermal conditions. Therefore, it should be observed quite generally for individual lamellae. In fact, picture-frame like morphologies of single crystals have been observed for a long time in polyethylene single crystals [23]. With the advent of AFM techniques direct observation of single crystal topography is possible. Evidence for rim-enhanced morphologies have been found by several groups [17,24–27]. In Fig. 14A and C we show an example for rim-enhanced morphologies obtained in experiments with short PS-PEO molecules crystallized from monolayers. Subsequent heating and annealing of the samples leads to further reorganization processes which will be discussed later.

To conclude this section we have shown that our lattice algorithm is able to predict experimental findings such as rim-enhanced morphologies of individual lamellae after annealing.

6. Morphogenesis of non-equilibrium growth patterns with internal reorganization

So far, we have considered isothermal growth and reorganization processes. Next, we will study the behavior of our model subjected to a jump in temperature as displayed in the temperature protocol in Fig. 15.

Instead of a simple melting scenario the temperature jump results in the morphogenesis presented in Fig. 16. After a short time, annealing leads to a hole-rim morphology which is most pronounced at about 3.6 TMS. Because of the high temperature the mobility of chains in the center of the fingers has increased dramatically. Chains at the rim, however, are already in a more stable state and persist. The latter serve now as nucleation sites for the reorganizing internal chains. Note the similarity with the experimental results shown in Fig. 14B and D, where the system was also subjected to a temperature jump followed by an annealing process. However, the temperature jump in Fig. 15 is too high for the hole-rim morphology to be stable. Already at about 9 TMS one observes degradation of the pattern. At a much longer time scale another morphological phase emerges which consists of droplets containing fully extended chains. Slow coalessence and ripening processes of the droplet phase can be seen on very long time scales. Within the available computational time melting is not observed. The temperature jump has resulted in morphogenesis with a much more stable pattern at the end.

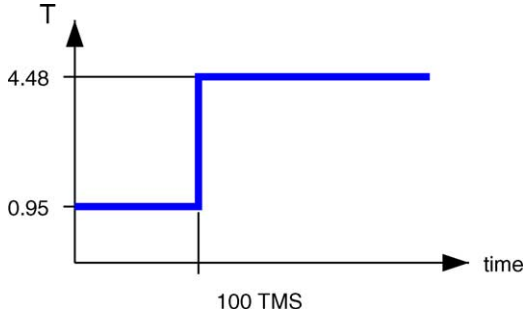

Fig. 15. Temperature protocol applied to the non-equilibrium growth pattern shown in Figs. 12 and 13.

In Fig. 17 we have plotted the internal energy of the system as a function of time. Note that the internal energy can be directly obtained from microscopic information, see Eq. (4), while entropy is not a priori available for non-equilibrium states. The high temperature jump causes an increase in internal energy at short times which corresponds to normal thermodynamic behavior. However, the formation of a hole-rim morphology is related to a normal decrease in internal energy. The break-up of hole-rim morphology leads again to an increase is internal energy but eventually the formation of the droplet phase results again in a decreasing internal energy. This is an excellent example for the complex response of a non-equilibrium system to an external perturbation.

In Fig. 18 the liquid fraction of the system is plotted as function of time after heating. It displays a monotonously increasing behavior which gives no indication for macroscopic melting-recrystallization processes. We note that the fraction of fully extended chains shows again a non-monotonous behavior which is complementary to that of the internal energy. This fact supports the role of molecular reorganization (in the crystalline state) during annealing of a polymer lamella.

The results of our lattice model concurs with direct observations during annealing after heating of monolayer crystals. In Fig. 19 we show results of one-step heating experiments on PEO. The annealing process after the temperature jump yields to a droplet-like phase with pronounced rim structures. This mixed (rim-droplet) phase presumably results from a

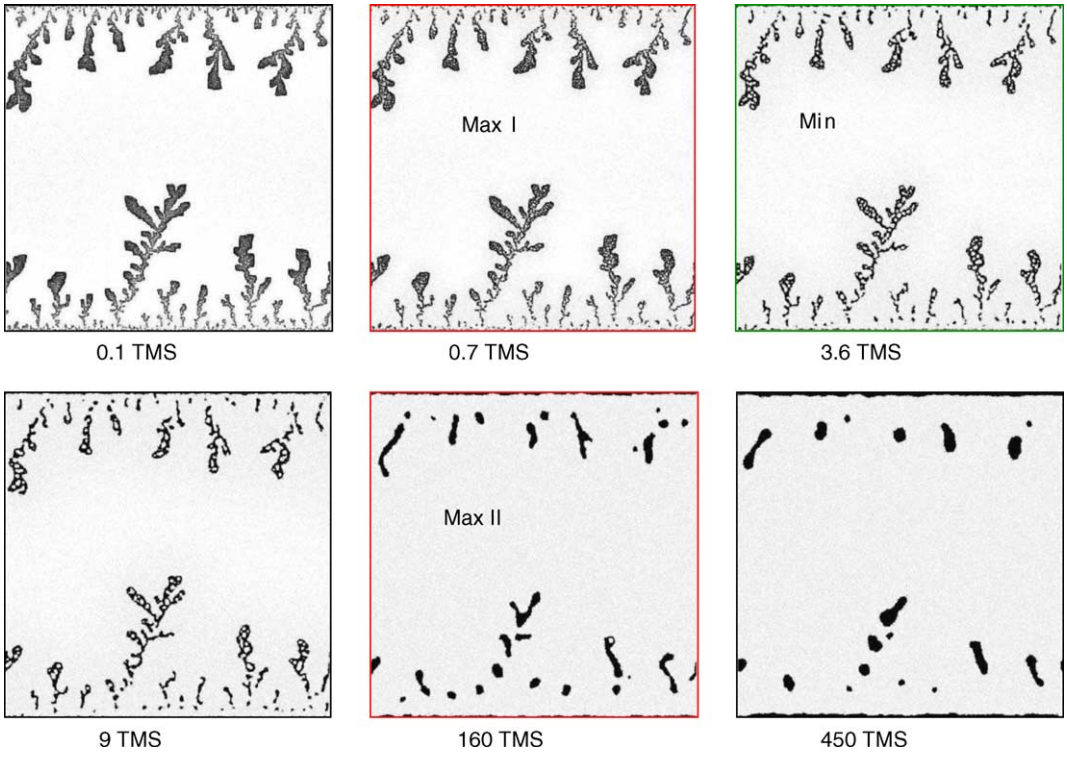

Fig. 16. Morphogenesis of a non-equilibrium growth pattern after the temperature jump shown in Fig. 15. Snapshots taken at the times (in TMS) indicated.

higher kinetic barrier against ordering and a relatively low temperature jump when compared to simulations.

To conclude this section we have shown that non-equilibrium growth patterns respond to temperature jumps with a complex morphogenesis instead of a direct melting process. The morphogenesis is driven by the interplay between (internal) chain ordering and (external) morphological features (number of nearest neighbors, growth morphology). Several meta-stable phases are obtained which are related to a non-monotonous behavior of thermodynamic observables such as the internal energy.

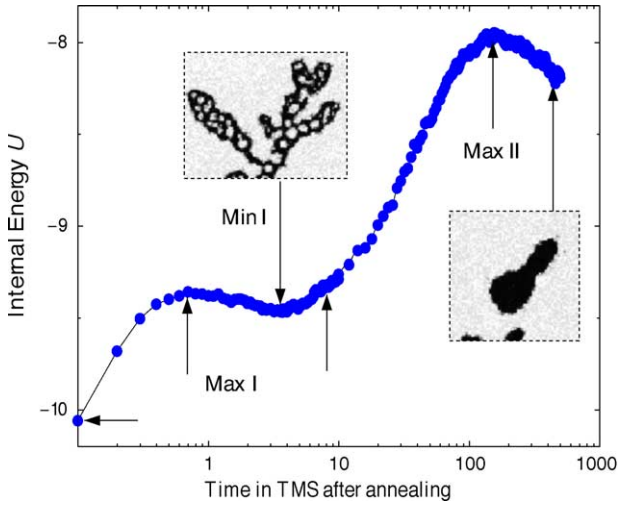

Fig. 17. Internal energy as a function of time corresponding to the morphogenesis in Fig. 16. The appearance of typical morphological patterns (snapshots in Fig. 16) is indicated by arrows.

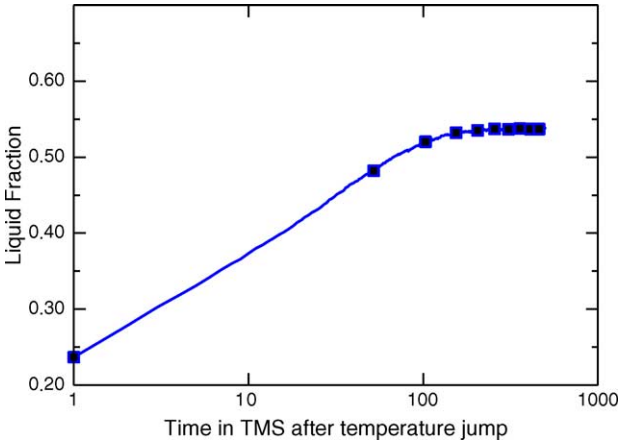

Fig. 18. Liquid fraction as a function of time after the temperature jump.

7. Non-equilibrium melting and heat capacity

In order to investigate the melting process of non-equilibrium crystals, we simulate a continuous heating rate according to a temperature protocol sketched in Fig. 20. We use again the system crystallized at $T = 0.95$ and $p_S = 0.6$ for 100 TMS, displayed in Fig. 13. Instead of a single big temperature jump we now continuously apply tiny jumps of $\Delta T = 0.01$ after each time interval Δt. The values used for

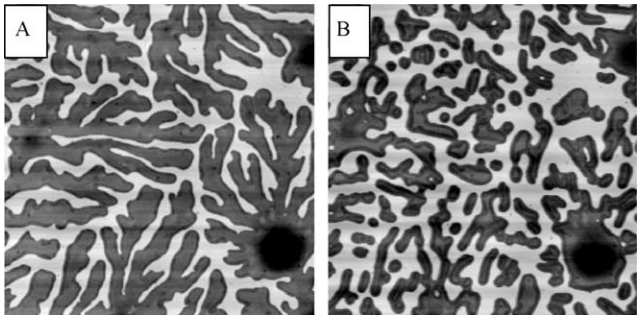

Fig. 19. Morphological transformations in a mono-lamellar crystal of PEO-7.6k grown at 35 °C for 10 min (A) before and (B) after the sample was annealed for 5 min at 45°C. The size of the images is 5 μm × 5 μm. Note the tendency for transformation of the tree-like shape of the fingers into an arrangement of droplet-like structures with a slightly higher region at the periphery. The defect zone at the right lower corner served as a marker for an unambiguous identification of the investigated area even after annealing.

Δt are 0.1, 0.5 and 5.0 TMS, respectively. This results in heating rates of 0.1, 0.02 and 0.002 TMS^{-1} in our units of the temperature.

In analogy to Fig. 17 we plot the response of the internal energy in Fig. 21 as a function of the temperature change ΔT. Because of the tiny temperature steps taken there is no rapid increase of internal energy as we have observed in Fig. 17 for the high temperature jump. Instead, we find a direct *decrease* of the internal energy as a response to the *increase* in temperature. This indicates anomalous thermodynamic behavior related to a *negative* heat capacity $C_V(T)$. Only at high temperatures normal behavior sets in which indicates ongoing melting of the system.

It is intriguing to consider directly the non-equilibrium heat capacity defined as

$$C_V = \frac{\mathrm{d}U}{\mathrm{d}T}. \tag{11}$$

The result is plotted in Fig. 22. For higher heating rates a relaxation process (minimum in C_V) is followed by continuous melting (increase or shallow maximum in C_V).

A particular behavior is shown for the lowest heating rate used in our simulations. Here, reorganization leads to a first peak in the heat capacity before the melting peak. Such double peaked behavior of the melting endotherm is frequently

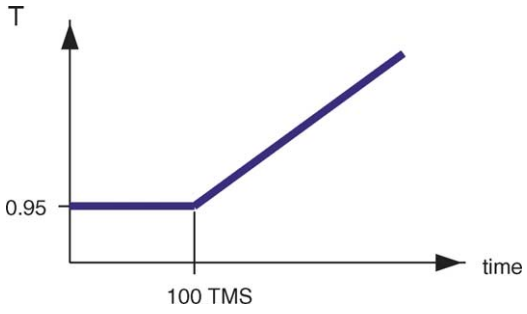

Fig. 20. Temperature protocol applied to the non-equilibrium growth pattern shown in Figs. 12 and 13.

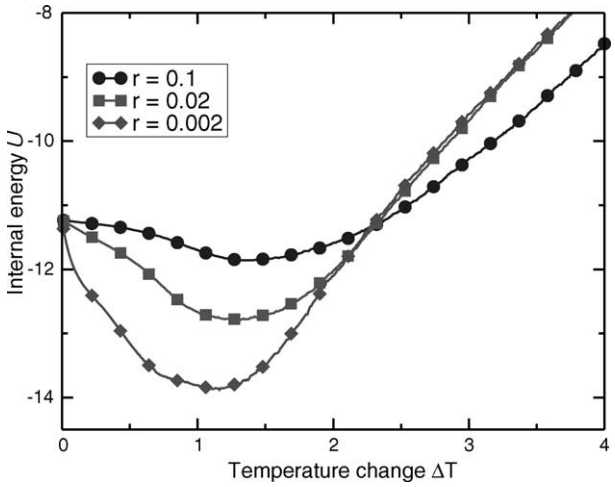

Fig. 21. Internal energy as a function of temperature change. The system has been crystallized at $T = 0.95$, $p_S = 0.6$ for 100 TMS. The heating rate r is given in TMS^{-1}, using our temperature units, see Eq. (6).

observed in the fusion of polymers. The conventional interpretation of this effect is *pre-melting* of less stable parts of crystalline morphology. In order to analyse this hypothesis we plot the liquid fraction for the lowest heating rate in Fig. 23. We can observe that the liquid fraction is decreasing until heating up to about $\Delta T = 0.45$. This rather indicates a continuation of the growth and crystallization processes instead of pre-melting. We conclude that the first peak is simply the consequence of the non-linear character of the morphogenetic processes. It indicates an accelerated reorganization (improvement of order) after the annealing temperature has reached a sufficiently high value. Note that the minimum of the liquid fraction nearly coincides with the minimum of the non-equilibrium heat capacity in Fig. 22.

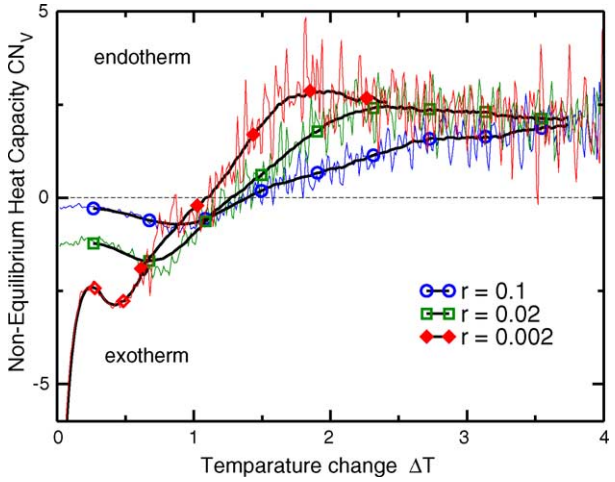

Fig. 22. Plot of the non-equilibrium heat capacity. The data are obtained by formal derivation of the energy function in Fig. 21 (thin lines) and are smoothed using a spline algorithm (thick lines and symbols).

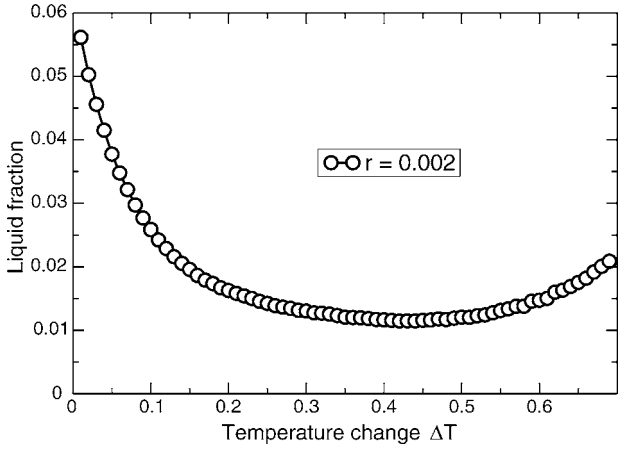

Fig. 23. Fraction of liquid chains as a function of the temperature change during heating for the lowest heating rate.

8. Conclusions

We have developed a coarse grained lattice model for polymer crystallization in ultra-thin films which assumes a cooperative behavior of the individual chains in all stages of the crystallization and melting process of polymers. Our model is able to describe reorganization processes of chains in the crystal which explains morphological changes during heating and annealing as observed in AFM experiments. We show that melting of non-equilibrium structures passes through a complex morphological pathway. The final melting process is not directly related to the structure formed at the crystallization temperature. If the heating process is very slow this results in a complex thermodynamical response of the system. The heat capacity, formally derived from the non-equilibrium internal energy, displays a double peak behavior as it is also observed in experiments. Based on the examination of complementary quantities such as the liquid fraction we have to exclude a simple interpretation in terms of melting-recrystallization processes. This shows for the first time that complex melting endotherms of polymer crystals are related to non-equilibrium reorganization and emphasizes the role of meta-stability in polymer crystallization.

References

[1] A. Keller, Phil. Mag. 2 (1957) 1171.
[2] P.H. Till, J. Polym. Sci. 24 (1957) 301.
[3] E.W. Fischer, Z. Naturf. A 12 (1957) 753.
[4] J.D. Hoffmann, G.T. Davis, J.I. Lauritzen, The Rate of Crystallization of Linear Polymers with Chain, vol. 3, Folding Plenum Press, 1976, pp. 497–614.
[5] B. Wunderlich, Macromolecular Physics, vol. 2, Nucleation, Crystallization, Annealing, Academic Press, New York, 1976.
[6] O.I. Paynter, D.J. Simmonds, M.C. Whiting, J. Chem. Soc. Chem. Commun. 1982 (1982) 1165.
[7] S. Rastogi, M. Hikosaka, H. Kawabata, A. Keller, Macromolecules 24 (1991) 6384.
[8] P. Bridgeman, Rev. Mod. Phys. 22 (1950) 56.
[9] M. Al-Hussein, G. Strobl, Polymer Crystallization: Observations, Concepts and Interpretations, vol. 606, in: J.-U. Sommer, G. Reiter (Eds.), Lecture Notes in Physics, Springer, 2003, Chapter 3.
[10] L. Mandelkern, Crystallization of Polymers: Equilibrium Concepts, Cambridge University Press, Cambridge, UK, 2002.
[11] A. Keller, E. Martuscelli, D. Priest, J. Polym. Sci. A-2 9 (1971) 1807.
[12] D.M. Sadler, Nature 326 (1987) 174.
[13] G. Ungar, P.K. Mandal, P.G. Higgs, D.S.M. de Silva, E. Boda, C.M. Chen, Phys. Rev. Lett. 85 (2000) 4397.
[14] J.-U. Sommer, Polymer 43 (2002) 929.
[15] M. Despotopoulou, C. Frank, R. Miller, J. Rabolt, Macromolecules 29 (1996) 5797.
[16] G. Reiter, J.-U. Sommer, Phys. Rev. Lett. 80 (1998) 3771.
[17] G. Reiter, J.-U. Sommer, J. Chem. Phys. 112 (2000) 4376.
[18] S. Miyashita, Y. Saito, M. Uwaha, J. Phys. Soc. Japan 66 (1997) 929.
[19] M. Uwaha, Y. Saito, Phys. Rev. A 40 (1989) 4716.
[20] T. Yamamoto, J. Chem. Phys. 107 (1997) 2653.
[21] J.-U. Sommer, G. Reiter, J. Chem. Phys. 112 (2000) 4384.
[22] J.-U. Sommer, G. Reiter, Phase Transitions 77 (2004) 703.
[23] D.A. Blackadder, H.M. Schleinitz, Polymer (7) (1966) 603.
[24] J. Hobbs, M. Hill, P. Barham, Polymer 41 (2000) 8761.
[25] A.K. Winkel, J.K. Hobbs, M.J. Miles, Polymer 41 (2000) 8791, crystallization, rim thickening, *n*-alkanes.
[26] M.W. Tian, J. Loos, J. Polym. Sci. B 39 (2001) 763.
[27] E.-Q. Chen, A.J. Jing, X. Weng, P. Huang, S.-W. Lee, S.Z.D. Cheng, B.S. Hsiao, F. Yeh, Polymer 44 (2003) 6051.